Carbon-13 NMR of Citrinin in the Solid State and in Solutions

R. Poupko and Z. Luz*

The Weizmann Institute of Science, 76100 Rehovot, Israel

R. Destro

Dipartimento di Chimica Fisica ed Elettrochimica e Centro CNR, via Golgi 19, 20133 Milan, Italy

Received: February 20, 1997; In Final Form: April 29, 1997[⊗]

Carbon-13 NMR is used to study the tautomeric equilibrium of citrinin in the solid state. The results confirm earlier X-ray diffraction studies, which indicated that the compound crystallizes in a disordered structure, with the *p*-quinone and *o*-quinone forms in a dynamic equilibrium. Analysis of the NMR data yields the equilibrium constant $K(T) = [o]/[p] = \exp(4.2/R)\exp(-1610/RT)$ (where R is in cal mol^{-1} K^{-1}), which is essentially identical to that determined by X-ray. The tautomerism is extremely fast on the NMR time scale ($>10^6$ s^{-1}). In methylene chloride solution citrinin also exists as a fast interconverting mixture of the two isomers with an equilibrium constant $K \sim 0.7$ at room temperature. However, the temperature dependence of the carbon-13 and oxygen-17 chemical shifts gave conflicting results, thus preventing a reliable determination of the thermodynamic parameters of K. In methanol and methanol/methylene chloride mixtures, citrinin undergoes a nucleophilic, Michael type, addition. The reaction is reversible, and the equilibrium shifts toward the normal cirtrinin form upon increasing temperature and in methanol/methylene chloride mixtures with increasing methylene chloride fraction. Only normal citrinin is obtained on crystallization, even from neat methanol.

Introduction

Citrinin ((3*R-trans*)-4,6-dihydro-8-hydroxy-3,4,5-trimethyl-6-oxo-3*H*-2-benzopyran-7-carboxylic acid) is a metabolite, produced by the fungus *Penicillium citrinum* and by several *Aspergillus* species. It has attracted much interest because of its antibiotic activity and as a suitable system to study biosynthetic pathways by isotopic labeling.[1−4] The chemical structure of citrinin including the absolute configuration of its asymmetric centers has been determined many years ago by chemical and spectroscopic methods.[5−10] Yet the problem of the tautomeric equilibrium between the *p*-quinone methide and *o*-quinone methide forms in solution has, so far, not been specifically addressed, although it is generally assumed to be in favor of the *p*-form.

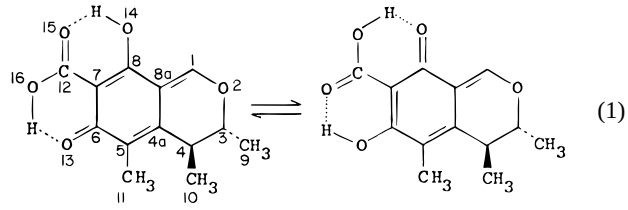

(1)

The equivalent problem in solid citrinin has, however, extensively been dealt with. The earliest study is by Rodig et al.,[11] who determined the crystal and molecular structure of crystalline citrinin by X-ray diffraction. By considering the interatomic distances in the molecule, they concluded that the compound crystallizes entirely in the *p*-quinone form. This interpretation was questioned by Sankawa et al.,[4] who suggested, on the basis of similar experiments, that citrinin exists "as a resonance hybrid between the two extreme structures", *p*-quinone and *o*-quinone. On the basis of oxygen-17 NMR data Sankawa et al. also suggested that the same situation applies to citrinin solutions. The problem was taken up again by Destro, who performed extensive X-ray measurements of crystalline citrinin in the temperature range 20 K to room temperature.[12−14] His results showed unequivocally that in solid citrinin both tautomers exist in equilibrium, which is temperature dependent, with the *p*-quinone form favored at low temperatures. By calculating accurate difference electron-density maps for the hydroxyl hydrogens involved in the tautomeric hydrogen shift, the following parameters for the *o*-quinone/*p*-quinone equilibrium constant

$$K = \frac{[o]}{[p]} = e^{-\Delta H/(RT)} e^{\Delta S/R} \qquad (2)$$

were determined, $\Delta H = 1.6 \pm 0.6$ kcal/mol, $\Delta S = 4.5 \pm 2.2$ eu.[13]

In the present work we extend the study of the tautomeric equilibrium of citrinin in the solid state using NMR spectroscopy. The NMR method is most suitable to study tautomeric equilibria[15] and has been extensively used both in solutions and in solid systems.[16] It is based on the fact that the chemical shifts, δ^i_A and δ^i_B of a particular nucleus, i, are different in the two interconverting tautomers, A and B. When the interconversion rate is much faster than the chemical shift difference, $k \gg 2\pi\nu_o|\delta^i_A - \delta^i_B|$, as is the case for solid citrinin, the NMR spectrum will consist of a single set of peaks at the weighted average chemical shift of the various nuclei,

$$\langle\delta^i\rangle = [A]\delta^i_A + [B]\delta^i_B \qquad (3)$$

Thus, if the chemical shifts of the isolated tautomers are known (and recalling that $[A] + [B] = 1$) the equilibrium constant can directly be determined from the relation

[⊗] Abstract published in *Advance ACS Abstracts,* June 15, 1997.

S1089-5639(97)00681-6 CCC: $14.00

$$K = \frac{[B]}{[A]} = \frac{\delta^i_A - \langle\delta^i\rangle}{\langle\delta^i\rangle - \delta^i_B} \quad (4)$$

To study the tautomeric equilibrium in solid citrinin, we use carbon-13 MAS NMR at high fields (7.05 and 11.74 T). We find a single set of peaks with chemical shifts that are slightly, but reproducibly, temperature dependent. We attribute this temperature dependence to a shift in the [*o*-quinone]/[*p*-quinone] ratio, and we use it to derive thermodynamic parameters for the equilibrium constant. We also report on the proton and carbon-13 NMR spectra of citrinin in methylene chloride and in methanol solutions. While in CH_2Cl_2 citrinin appears to have a similar structure as in the solid state, in methanol and in methanol/methylene chloride mixtures it exists as an equilibrium mixture of the normal form and a methanol−citrinin adduct formed by a nucleophilic addition of solvent molecules.

Experimental Section

Carbon-13 spectra of crystalline citrinin at natural isotopic abundance were recorded by the cross-polarization magic angle spinning (CPMAS) method, using a contact time of 4 ms and a recycle time of 10 s. Two sets of experiments were performed at 75.46 and 125.8 MHz using Bruker CXP300 (at the Weizmann Institute) and ASX500 (at the Max-Planck-Institute for Polymer Research, Mainz) spectrometers. The rotors in the two spectrometers had diameters of 5 and 4 mm respectively and were packed with about 90 mg of citrinin. The rf power corresponded to $\pi/2$ pulses of 5.0 μs in the CXP300 and 3.6 μs in the ASX500 spectrometers. The final analysis of the results was made on data collected on the latter spectrometer, because of its higher resolution and better temperature control system. We did not calibrate the temperature unit during the experimental session, but from calibration performed subsequently on a similar probe head, using $Pb(NO_3)_2$ as reference,[17] we estimate a temperature uncertainty of no more than 2−3 K.

High-resolution spectra of ^{1}H, ^{13}C, and ^{17}O in solution were recorded by single-pulse excitation at, respectively, 500.13, 125.8, and 67.8 MHz, using a Bruker AM500 spectrometer, equipped with a BVT2000 temperature control unit. The temperature uncertainty in these experiments was less than 2 K. Various two-dimensional experiments were performed to confirm the proton and carbon-13 peak assignment, including ^{1}H−^{13}C chemical shift correlation, as well as ^{1}H and ^{13}C 2D exchange experiments. The solutions were prepared gravimetrically and contained about 2−3 wt % citrinin (except for the solution used to record the oxygen-17 spectrum, which contained 5 wt % of the compound).

Results and Discussion

A. Carbon-13 NMR of Solid Citrinin. Carbon-13 CPMAS NMR spectra of solid citrinin (Aldrich) were recorded as function of temperature at both 75.46 and 125.8 MHz. Both sets of results were essentially identical, but the accuracy of the higher frequency spectra, some of which are shown in Figure 1, was considerably better. The peak positions of these spectra are very close to those observed in a methylene chloride solution of citrinin, shown in the bottom trace of the figure. The peak assignment of the solution spectrum is based on earlier studies[1,4] and some further experiments to be discussed in the next section. Because of the similarity of the two types of spectra, the assignment of the solution spectrum was carried out to that of the solid. Although at first glance the solid state spectra appear to depend very little on temperature, close examination of the whole set of data reveals systematic changes. The chemical

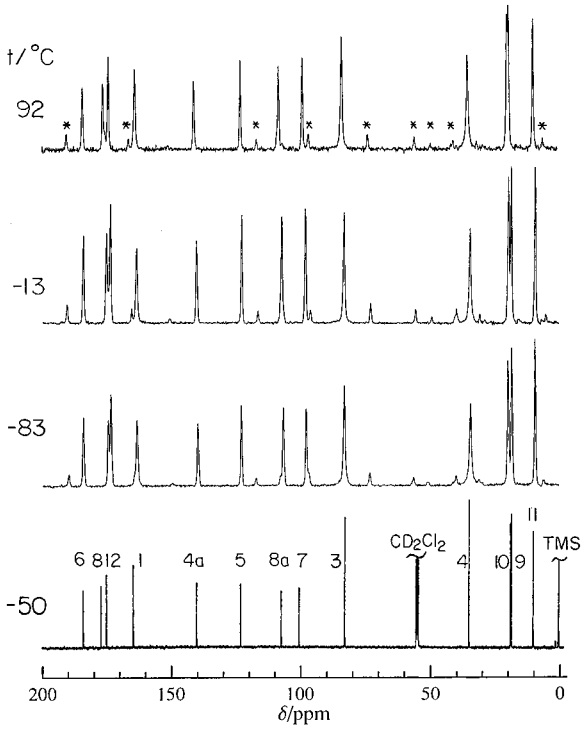

Figure 1. Top three traces: carbon-13 CPMAS spectra of solid citrinin at three different temperatures as indicated. The spectra were recorded at 125.8 MHz at a spinning frequency of 8.5 kHz. Number of scans 750, recycle time 10 s. The asterisks indicate spinning side bands. Bottom trace: High-resolution, proton-decoupled, ^{13}C spectrum in a 3 wt % solution of citrinin in methylene chloride at −50 °C, also recorded at 125.8 MHz. Number of scans 220, recycle time 3 s. The scale for all spectra is relative to TMS, and the peak assignment refers to the numbering system shown in text.

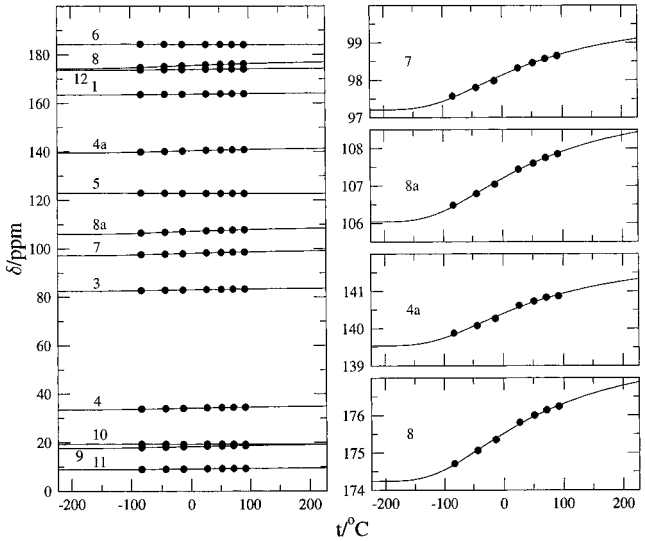

Figure 2. Left: Plots of the chemical shifts of all carbons in solid citrinin as function of temperature, derived from spectra of the type shown in Figure 1. The full curves are calculated as explained in the text. Right: Same as on the left diagram with a highly expanded vertical scale, for four of the carbons, which exhibit larger temperature dependent shifts.

shifts of all carbons are plotted on the left side of Figure 2 as function of temperature and for some of the nuclei (those with the larger temperature dependence) also on an expanded scale on the right side of the figure. The width of the various peaks (full width at half-maximum height) varied from 60 to 100 Hz (0.5−0.8 ppm), and the peak position could be determined to better than 0.08 ppm. It may be seen that some of the peaks

TABLE 1: Limiting Values of δ_p^i and δ_o^i for the Various Carbons of Citrinin in the Solid State[a]

carbon number	1	3	4	4a	5	6	7	8	8a	9	10	11	12
δ_p	163.43	82.54	33.51	139.54	122.96	184.31	97.21	174.24	106.04	17.61	19.32	8.82	173.56
δ_o	164.46	84.30	35.82	142.43	122.63	183.93	100.28	178.52	109.91	20.13	19.38	9.97	174.74
Δ[b]	1.03	1.76	2.31	2.89	−0.33	−0.38	3.07	4.28	3.87	2.52	0.06	1.15	1.18

[a] The numbering system is as given in the text. The entries are in ppm relative to TMS. [b] $\Delta = \delta_o - \delta_p$.

TABLE 2: Calculated δ_p^i and δ_o^i for Gas-Phase *p*- and *o*-Citrinin, by *ab Initio* CSGT Using a 6-31G* Basis Set (Ref 19)[a]

carbon number	1	3	4	4a	5	6	7	8	8a	9	10	11	12
δ_p	160.28	62.05	20.93	131.96	119.02	181.82	96.07	173.87	95.94	13.21	14.22	7.51	164.85
δ_o	163.92	61.80	21.03	140.31	108.65	179.86	96.14	178.92	100.75	13.07	14.22	6.88	165.10
Δ[b]	3.64	−0.25	0.10	8.35	−10.37	−1.96	0.07	5.05	4.81	−0.14	0.00	−0.63	0.25

[a] The entries are in ppm relative to methane. [b] $\Delta = \delta_o - \delta_p$.

are barely affected by the temperature, while others shift by as much as 2 ppm over the temperature range −90 to +90 °C.

Motivated by the X-ray results discussed above, we attempted to interpret these chemical shift changes in terms of a temperature dependent dynamic equilibrium between the *p*-quinone and *o*-quinone forms of citrinin. Since only one peak is observed for each carbon, we conclude that the interconversion of the two tautomers is fast on the NMR time scale and the changes in the chemical shifts reflect a shift in their equilibrium ratio with temperature. In principle we should therefore be able to derive the temperature dependence of the *o*-quinone/*p*-quinone ratio from the average shifts, $\delta^i(T)$, of the various carbons using eq 4, with A ≡ *p*-quinone and B ≡ *o*-quinone. The problem is that the limiting values, δ_p^i and δ_o^i, in the pure *p*-quinone and *o*-quinone forms are not known. It is also clear that they do not differ very much, and it would therefore be difficult to estimate their difference by chemical shift additivity rules. On the other hand, the accuracy of the measurements and the large experimental data set allow us to perform an overall best fit analysis in which the δ_o^i and the δ_p^i, as well as $K(T)$, are parameters to be determined by minimizing a suitable error function. Combining eqs 2 and 4 yields for each $\delta^i(T)$

$$\delta^i(T) = \frac{1}{1+K(T)}[K(T)\delta_o^i + \delta_p^i] = \left[1 + \alpha \exp\left(-\frac{\Delta H}{RT}\right)\right]^{-1}\left[\alpha \exp\left(-\frac{\Delta H}{RT}\right)\delta_o^i + \delta_p^i\right] \quad (5)$$

where $\alpha = \exp(\Delta S/R)$. There are 91 experimental points (13 measured δ^i's at 7 temperatures) to fit 28 parameters (13 δ_p^i's, 13 δ_o^i's, ΔS, and ΔH). In practice we first fitted the results for each carbon to eq 5. The values obtained for ΔH and ΔS from the various carbons, particularly those exhibiting relatively large temperature dependent shifts, were very close. Encouraged by these results we performed a global best fit analysis by minimizing the overall error function $\sum[\delta^i(T)^{\mathrm{exp}} - \delta^i(T)^{\mathrm{cal}}]^2$. The values so obtained for the δ_o^i and δ_p^i are summarized in Table 1, and the derived best fit thermodynamic parameters are

$$\Delta H = 1.61 \pm 0.02 \text{ kcal mol}^{-1} \qquad \Delta S = 4.2 \pm 0.9 \text{ eu}$$

where the error limits are standard deviations obtained from the overall set of the results. The actual uncertainty in these parameters is probably much higher since the analysis does not take into account possible changes of the chemical shift with the temperature due to effects other than tautomerism. Such changes may be nonnegligible in comparison to the experimentally observed shifts, but we have no way to estimate them. Our confidence in the interpretation stems from several facts, the foremost being the close similarity of the results with those derived independently by the X-ray diffraction method.[13] Also the facts that the temperature dependence of the chemical shifts could well be interpreted in terms of sigmoidal curves and that the carbons which undergo the largest shifts are associated with the tautomeric center of the molecule lend strong support to the assumed model and to the procedure used in analyzing the results.

We do not have independent experimental results against which the limiting chemical shift values of Table 1 may be compared. The differences, $\Delta^i = \delta_o^i - \delta_p^i$, are quite small; some are positive, others are negative. Some Δ's are relatively large, even though they correspond to atoms which are further away from the tautomeric center (e.g. Δ^9 and Δ^{4a}) than others, which are close but show only a small effect (e.g. Δ^6). Some support for the above results can, however, be derived by comparison with *ab initio* quantum chemical calculations. Such calculations, for citrinin in the gas phase, are currently in progress.[18] The main purpose of this study is to compare the optimized geometries and energies of the *p*- and *o*-forms of citrinin and to investigate possible transition states of the tautomeric equilibrium. We have used the optimized geometries and electronic wave functions for the free citrinin molecule (using CSGT with a 6-31G* basis set[19]) from this study to calculate the carbon-13 isotropic magnetic shieldings for the various atoms in both tautomeric forms. The results (in ppm downfield from methane) are summarized in Table 2. It may be seen that the calculated shielding constants for the para form are indeed quite similar to those of the ortho. Moreover the calculations give relatively large Δ values for some of the carbons which are remote from the tautomeric center as also found experimentally (e.g. Δ^{4a}), although for others they predict much too high values (e.g. Δ^5). The deviations are, however, within the range of reliability of the method.[20] We should also recall that the calculations are for the free molecules in the gas phase and do not include the effect of packing and of interaction with neighboring molecules.

Before discussion of the solution spectra of citrinin, a short comment on the rate of the tautomeric process in the solid state is in order. In principle it could be estimated from relaxation measurements as function of temperature, but such measurements were not carried out. A lower limit can be estimated from the fact that the widths of all lines are independent of temperatures. This indicates that there is essentially no contribution to $1/T_2$ from the proton exchange process. Setting an upper limit of 1 s^{-1} for this contribution yields a lower limit of 10^6 s^{-1} for the rate, but it could be (and probably is) much faster.

B. Carbon-13, Oxygen-17 and Proton NMR of Citrinin in Methylene Chloride Solutions. The carbon-13 NMR spectrum in methylene chloride (CD_2Cl_2) was already shown

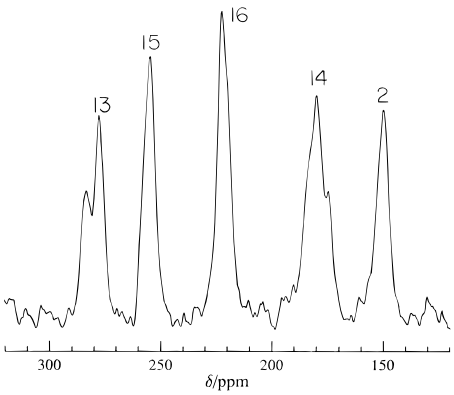

Figure 3. Oxygen-17 NMR spectrum of a 5 wt % solution of citrinin in methylene chloride at 37 °C. Number of scans 91 000, recycle time 0.1 s.

in Figure 1 (bottom trace). The assignment of the spectrum was taken from the work of Sankawa et al.[4] and Staunton,[1] who studied the NMR spectra of various biosynthetically enriched citrinin samples. The only change from Sankawa's more recent assignment is the switching of the labeling of peaks 10 and 11 as originally determined by Colombo et al.[3b] This is based on our $^1H-^{13}C$ 2D chemical shift correlation experiment, making use of the well-established proton peak assignments of Barber et al.[3a] The carbon-13 spectrum in methylene chloride consists of a single set of lines, as in the solid, indicating fast *p*-quinone/*o*-quinone interconversion. The shifts are slightly temperature dependent, ranging from −1.7 to +1.2 ppm between −70 and 58 °C, and in principle could be analyzed in terms of the *o*-quinone/*p*-quinone equilibrium, as was done for the solid. Such an analysis yields similar ΔH and ΔS values to those found in the solid, with $K \sim 0.75$ at around room temperature. However, we refrain from presenting a full analysis of these data because of conflicting results from the oxygen-17 NMR measurements described below.

For this nucleus we expect to observe much larger changes in the peak position upon changing the temperature. As is well-known the resonance frequencies of the carbonyl and hydroxyl oxygens differ quite considerably (by $\Delta^O = 450$ to 500 ppm).[21,22] Thus for a *p*-quinone/*o*-quinone equilibrium constant around unity, relatively large shifts are expected with temperature for the resonance frequencies of oxygens 13 and 14 (and likewise for oxygens 15 and 16). The chemical shifts of oxygens 13 and 14 (in an undisclosed solvent and presumably at room temperature) were recorded earlier[4] in a biosynthetically enriched sample of citrinin and found to fall at 279 and 179 ppm respectivley (relative to $H_2{}^{17}O$). Using eq 4 and the above estimates of δ_p and δ_o for carbonyl and hydroxyl oxygens, we find $K = 0.9$ and 0.45 from the resonances of oxygens 13 and 14 respectively. Although the average value, $K = 0.67$, is close to that determined from the carbon-13 results ($K = 0.75$), the fact that the two oxygens gave K values differing by a factor of 2 is disturbing. Even more puzzling is the observation that the oxygen-17 chemical shifts are essentially independent of temperature. We have recorded the oxygen-17 spectrum of a 5 wt % solution of normal (unenriched) citrinin in methylene chloride over the temperature range 7 to 47 °C. (Below 0 °C the lines are too broad to measure due to enhanced relaxation.) The spectrum at 37 °C is shown in Figure 3. The peaks due to oxygens 13 and 14 at 278 and 179 ppm are readily identified, as is also the peak due to oxygen 2 at 149 ppm (on the basis of ref 4). We can also safely identify the peaks at 255 and 222 ppm with, respectively, oxygen 15 and 16. The extra feature at 284 ppm and the structure of the 179 ppm peak (both of which are not affected by proton decoupling) are not clear. In the temperature range 7 to 47 °C, none of the lines shifts by more than 2.5 ppm, while from the equilibrium constants estimated from the carbon-13 results a shift of ∼40 ppm is predicted in the above temperature range for oxygens 13 and 14. Because of these discrepancies we withhold further discussion of the *p*-quinone/*o*-quinone equilibrium in methylene chloride solutions until the oxygen-17 chemical shift results are better understood.

It is interesting to note that the carboxylic oxygens 15 and 16 give separate signals over the entire temperature range, indicating that on the NMR time scale, the carboxyl group does not reorient about the C_7-C_{12} bond. This reflects the strong intramolecular hydrogen bonds which fix the double-ring structure of the carboxyl group. The proton NMR spectrum of citrinin in methylene chloride is consistent with this observation. Its structure is essentially the same as described by Barber et al.[3a] in $CDCl_3$; it exhibits one signal for each hydrogen, including (at low temperatures) two sharp peaks at 15.4 and 16.4 ppm due to the "hydroxy" and "carboxy" hydrogens in the double ring of the carboxylic group (see Table 3).

C. NMR Spectra of Citrinin in Methanol and Methanol/Methylene Chloride Mixtures. When citrinin is dissolved in methanol or in methanol/methylene chloride mixtures, a dramatic change in the solute NMR spectrum takes place. Examples of carbon-13 spectra of citrinin dissolved in neat CD_3OD and in a 1:3 volume mixture CD_3OD/CD_2Cl_2 at low temperatures (−55 °C) are depicted in Figure 4. For comparison the spectrum in neat CD_2Cl_2 is also shown. Referring to the spectrum in neat CD_3OD, two main effects may be observed: (i) Each carbon exhibits two peaks with relative intensities of ∼1:2.5. (ii) The peaks are shifted, some of them quite considerably, from their position in the methylene chloride solution. The peak position in methanol (at −60 °C) as well as in methylene chloride (at −70 °C) are listed in Table 3. Note in particular the large shift of carbon 1 by almost 70 ppm. Such a shift can only be due to a chemical transformation of the citrinin molecule. We ascribe it to a 1−4, Michael type, nucleophilic addition of methanol to the *o*-quinone form of citrinin

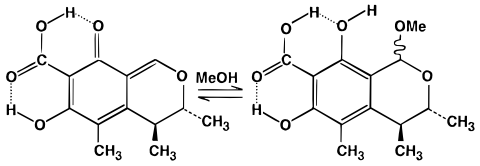

Such a process will strongly affect the chemical shift of carbon 1, which transforms from an olephinic to aliphatic atom, as indeed observed experimentally. The reaction shifts the *o*-quinone/*p*-quinone equilibrium toward the *o*-quinone form and the doubling of the signals is ascribed to the two epimeric forms with the OMe group either cis or trans to the methyl-10 group at carbon 4 as indicated by the wiggly bond. The spectra shown in Figure 4 were recorded in CD_3OD and CD_3OD/CD_2Cl_2 mixtures. When spectra are recorded in CH_3OD or CH_3OD/CD_2Cl_2 mixtures an additional pair of peaks is observed at around 55 ppm as shown by the insert in the bottom trace of Figure 4. These peaks are ascribed to the methoxy carbons bound to carbon 1 in the adduct. Their signals in CD_3OD are apparently too weak to observe, due to the lack of Overhauser enhancement and excessive splitting by the three methyl deuterons of the OCD_3 group.

The addition reaction is reversible and shifts toward free citrinin with increasing temperature and/or the fraction of methylene chloride in mixed methanol/methylene chloride

TABLE 3: Carbon-13 (Top) and Proton (Bottom) Chemical Shifts of Citrinin and the Citrinin−Methanol Adduct in Methanol and Methylene Chloride Solutions, Respectively[a]

solvent		1	3	4	4a	5	6	7	8	8a	9	10	11	12	CH_3O[d]
CD_3OD (−60 °C)	δ_A	95.77	69.64	38.04	147.76	114.67	160.58	97.95	156.91	113.48	20.54	19.10	12.45	173.14	55.17
	δ_B	95.46	74.02	36.05	146.35	114.14	160.26	98.65	157.89	111.34	22.30	19.10	10.02	173.32	55.28
CD_2Cl_2 (−70 °C)		164.96	82.49	34.47	140.13	123.02	184.00	100.00	177.02	107.03	18.26	18.69	9.98	175.07	
CD_3D[b] (−60 °C)	δ_A	5.50	3.87	2.67							1.34	1.17	2.02		3.51
	δ_B	5.42	4.08	2.80							1.32	1.18	2.05		3.54
CD_2Cl_2[c] (−70 °C)		8.40	4.90	3.08							1.35	1.21	2.02		

[a] A and B refer, respectively, to the more and less abundant isomers of the methanol adduct. The shifts are in ppm relative to TMS. [b] In addition two pairs of peaks at (A) 10.74, 11.12 and (B) 11.13, 10.96 ascribed to the hydroxy and carboxyl hydrogens in the two isomers are observed in CH_3OH and CH_3OH/CD_2Cl_2 mixtures at low temperatures. The chemical shifts quoted are for a 1:1 methanol/methylene chloride solvent at −80 °C. [c] In addition two peaks at 15.29 and 16.36 due to the hydroxy and carboxy hydrogens in the double-ring structures of the carboxylic group are observed. [d] These peaks are only observed in solvents containing CH_3OD or CH_3OH.

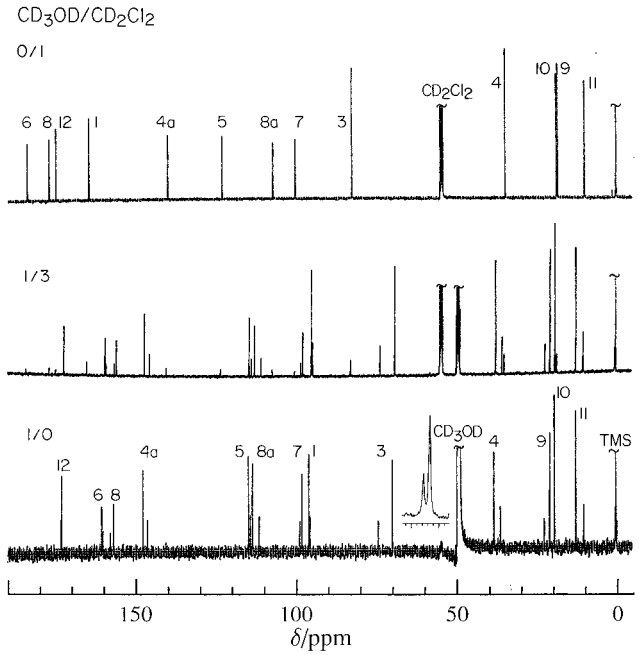

Figure 4. Carbon-13 NMR spectra of a saturated solution of citrinin in neat methanol (bottom), in a 1:3 volume mixture of CD_3OD/CD_2Cl_2 (2.1 wt % citrinin) (middle) and in neat CD_2Cl_2 (3.0 wt %) (top), at −55 °C. The assignments in the top spectrum are as in the bottom trace of Figure 1 and correspond to the normal form of citrinin. The assignments in the bottom spectrum correspond to the A and B isomers of the methanol adduct. The insert shows the two CH_3O signals observed when CH_3OD is used instead of CD_3OD in the range 55.5−55.0 ppm (larger ticks in the inserted scale). The middle spectrum exhibits peaks due to both normal citrinin and its methanol adduct.

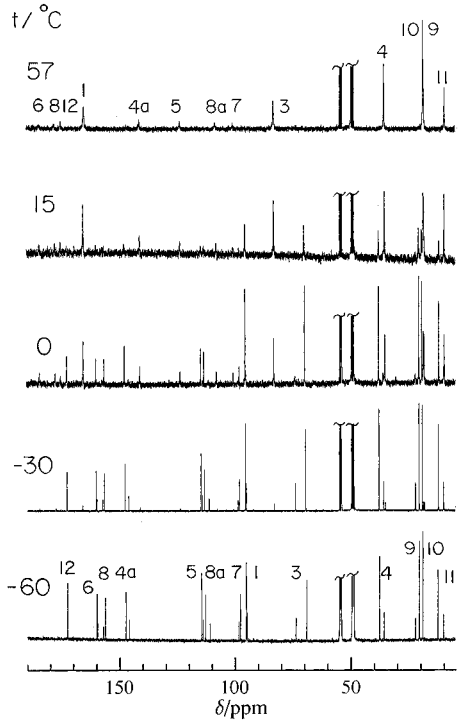

Figure 5. Carbon-13 NMR spectra in a 2.1 wt % solution of citrinin in a 1:1 volume mixture of CD_3OD/CD_2Cl_2 at the indicated temperatures. The peak assignments are as in Figure 4.

solvents. This may be clearly seen in Figures 4 and 5. In the middle trace of Figure 4, which corresponds to a CD_3OD/CD_2Cl_2 mixture of 1/3 at −55 °C, two sets of peaks are observed due to the adduct and the normal citrinin form. In fact the assignment of the adduct signals was established by a 2D exchange experiment performed on this solution at −30 °C (using a mixing time of 4 s). For each signal of normal citrinin two cross-peaks were observed with the corresponding signals of the cis/trans isomers of the adduct, thus providing an assignment for the spectrum of the latter. The experiment also provides a time scale for the interconversion rate (∼2.5 s^{-1} at −30 °C).

Figure 5 depicts spectra recorded in a 1:1 CD_3OD/CD_2Cl_2 mixture as a function of temperature. They show the gradual shift of the equilibrium from the adduct to the normal form of citrinin with increasing temperature. At −60 °C there are only signals due to the adduct; at −30 and 0 °C two sets of peaks are observed due to the adduct and the normal form, while at 15 and 57 °C predominantly signals due to normal citrinin are detected. In the latter spectra, however, the signals are broadened by the fast reversible methanol addition. This indicates the presence of a finite concentration of adduct even at the higher temperatures, but because of its low concentration and correspondingly broader peaks its signals are too weak to observe. We have not studied the interconversion kinetics quantitatively, but from the line widths of the signals at room temperature in the 1:1 CD_3OD/CD_2Cl_2 mixture a life time of 12 ms for the normal citrinin form can be estimated.

The same general behavior is also observed in the proton NMR spectra of citrinin. In CD_2Cl_2 a single signal is observed for each hydrogen, while in methanol and methanol/methylene chloride mixtures at low temperatures the spectrum is doubled and shifted from that in CD_2Cl_2. The low-temperature chemical shifts in both solvents are included in Table 3. Again the largest shift is exhibited by hydrogen 1 (from 8.4 ppm in CD_2Cl_2 to ∼5.5 ppm in methanol). When the spectrum is recorded in CH_3OH or CH_3OD two additional peaks at 3.51 and 3.54 ppm are observed due to the methoxy hydrogens of the two adduct isomers. When CH_3OH (or CD_3OH) is used as solvent, two pairs of low-field peaks are also observed which are ascribed to the hydrogens in the double ring of the carboxyl group in the two adduct isomers. As for carbon-13 the proton spectra

too show a shift in the adduct/normal citrinin equilibrium as a function of the temperature and the methanol/methylene chloride ratio. Also dynamic line broadening due to exchange between the two forms of critinin was observed with increasing temperature. However, we have not studied these effects quantitatively.

The sensitivity of carbon 1 toward nucleophiles is consistent with an earlier observation[3c] in which citrinin was reacted with alkali to cleave the dihydropyrane ring. Such a reaction involves a nucleophilic attack at carbon 1. Also, in the recent study on the charge density in citrinin[14b] the chemical reactivity of site 1 toward nucleophiles is confirmed by the shape of the molecular reaction surface.

Summary and Conclusions

We have presented a detailed study of the temperature dependence of the carbon-13 chemical shifts in solid citrinin by CPMAS spectroscopy. In the temperature range −90 to +90 °C small but reproducible shifts were observed which could be quantitatively interpreted in terms of the dynamic equilibrium between the *p*-quinone and *o*-quinone forms of citrinin. The thermodynamic parameters obtained for the equilibrium constants are in full agreement with earlier results derived from X-ray diffraction.[13]

An attempt to use the same method to determine the *p*-quinone/*o*-quinone equilibrium in methylene chloride solution was frustrating because of conflicting results from carbon-13 and oxygen-17 measurements. The oxygen-17 spectra of citrinin in methylene chloride indicate that the equilibrium is of order unity and changes very little around room temperature. Quantum mechanical calculations on citrinin molecules in the gas phase indicate that the two forms have nearly the same energy.[18] The exact values of the equilibrium constants in the various systems must therefore depend to a large extent on external factors such as solvation and hydrogen bonding in solutions and packing forces and intermolecular interactions in the solid.

A completely different behavior is observed for citrinin in methanol and methanol/methylene chloride solutions. Here citrinin undergoes a nucleophilic addition by methanolate ions resulting in a well-defined adduct, consisting of a mixture of two isomeric species. The equilibrium, adduct/normal citrinin, is reversible, and the interconversion is very fast at room temperature. The equilibrium is also strongly dependent on the solvent composition and on the temperature; increasing the methylene chloride fraction in the methanol/methylene chloride mixtures and raising the temperature shifts the equilibrium toward free citrinin, while in methanol-rich mixtures and low temperatures the concentration of the adduct dominates. The adduct is, however, only stable in solution. Crystallization from neat methanol yields free citrinin with the same crystal structure as that obtained by crystallization from ethanol, used in the X-ray measurements.[12−14]

Acknowledgment. We thank Professors H.-H. Limbach (Berlin) and Charles L. Perrin (UC San Diego) for proposing the formation of the adduct in the methanol solution and many other valuable comments on an earlier version of the paper. We also thank Professor H.W. Spiess and Dr. S. Koebler for allowing the use of their ASX500 spectrometer. This work was partly supported by a grant from the United States-Israel Binational Science Foundation (BSF), Jerusalem, Israel.

References and Notes

(1) Barber, J.; Staunton, J. *J. Chem. Soc., Chem. Commun.* **1979**, 1098.
(2) Barber, J.; Staunton, J. *J. Chem. Soc., Chem. Commun.* **1980**, 552.
(3) (a) Barber, J.; Carter, R. H.; Garson, M. J.; Staunton, J. *J. Chem. Soc., Perkin Trans. 1* **1981**, 2577. (b) Colombo, L.; Gennari, C.; Severini Ricca, G.; Scolastico, C.; Aragozzini, F. *J. Chem. Soc., Perkin Trans. 1* **1980**, 675. (c) Colombo, L.; Gennari, C.; Potenza, D.; Scolastico, C.; Aragozzini, F.; Merendi, C. *J. Chem. Soc., Perkin Trans. 1* **1981**, 2594.
(4) Sankawa, U.; Ebizuka, Y.; Noguchi, H.; Isikawa, Y.; Kitaghawa, S.; Yamamoto, Y.; Kobayashi, T.; Iitak, Y. *Tetrahedron* **1983**, *39*, 3583.
(5) (a) Brown, J. P.; Robertson, A.; Whalley, W. B.; Cartwright, N. J. *J. Chem. Soc.* **1949**, 867. (b) Cartwright, N. J.; Robertson, A.; Whalley, W. B. *J. Chem. Soc.* **1949**, 1563. (c) Johnson, D. H.; Robertson, A.; Whalley, W. B. *J. Chem. Soc.* **1950**, 2971.
(6) Cram, D. J. *J. Am. Chem. Soc.* **1950**, *72*, 1001.
(7) Kovac, G.; Nemec, P.; Betina, B.; Balan, J. *Nature (London)* **1961**, *190*, 1104.
(8) Mathieson, D. W.; Whalley, W. B. *J. Chem. Soc.* **1964**, 4640.
(9) Mehta, P. P.; Whalley, W. B. *J. Chem. Soc.* **1963**, 3777.
(10) Hill, R. K.; Gardella, L. A. *J. Org. Chem.* **1964**, *29*, 766.
(11) Rodig, O. R.; Shiro, M.; Fernando, Q. *J. Chem. Soc., Chem. Commun.* **1971**, 1553.
(12) Destro, R.; Marsh, R. E. *J. Am. Chem. Soc.* **1984**, *106*, 7269.
(13) Destro, R. *Chem. Phys. Lett.* **1991**, *181*, 232.
(14) (a) Destro, R.; Merati, F. *Z. Naturforsch.* **1993**, *48a*, 99. (b) Roversi, P.; Barzaghi, M.; Merati, F.; Destro, R. *Can. J. Chem.* **1996**, *74*, 1145.
(15) An extensive review of enol tautomerism may be found in: Gilli, G., Bertolasi, V. *The Chemistry of Enols*; Rappoport, Z., Ed.; John Wiley and Sons: New York, 1990; Chapter 13, p 713.
(16) Limbach, H.-H. In *NMR Basic Principles and Progress*; Springer-Verlag: Berlin, 1990; Vol. 23, p 63.
(17) Bielecki, A.; Burum, D. P. *J. Magn. Reson., Ser. A* **1995**, *116*, 215.
(18) Barzaghi, M.; Merati, F.; Roversi, P.; Destro, R. Unpublished results.
(19) Keith, T. A.; Bader, R. F. W. *Chem. Phys. Lett.* **1992**, *194*, 1. Keith, T. A.; Bader, R. F. W. *Chem. Phys. Lett.* **1993**, *210*, 223.
(20) Cheeseman, J. R.; Trucks, G. W.; Keith, T. A.; Frisch, M. J. *J. Chem. Phys.* **1996**, *104*, 5497.
(21) Gorodetzky, M.; Luz, Z.; Mazur, Y. *J. Am. Chem. Soc.* **1967**, *89*, 1183.
(22) Boykin, D. W.; Baumstark, A. L. *Tetrahedron* **1989**, *45*, 3613. Chandrasekaran, S.; Wilson, W. D.; Boykin, D. W. *Org. Magn. Reson.* **1984**, *22*, 757.